Progress In Electromagnetics Research, Vol. 175, 81–89, 2022

Deep Learning Approach Based Optical Edge Detection Using ENZ Layers

Yifan Shou[1, 2, 3], Yiming Feng[1, 2, 3], Yiyun Zhang[1, 2, 3], Hongsheng Chen[1, 2, 3, *], and Haoliang Qian[1, 2, 3, *]

(*Invited*)

Abstract—Metamaterials offer a chance to design films that could achieve optical differentiation due to their special properties. Layered film would be the simplest case considering the easy-fabrication and compactness. Instead of performing the optical differentiation at the Fourier plane, Green-function based multi-layers are used to achieve optical differentiation. In this work, epsilon-near-zero (ENZ) material is utilized to realize the optical differentiation owning to the special optical properties that the reflection increases with the increase of incident angle, which fits the characteristics of optical differentiation. In addition, deep learning is also used in this work to simplify the design of ENZ layers to achieve the optical differentiation, and further realize the optical edge detection. Simulations based on the Fresnel diffraction are carried out to verify that our films designed by this method could realize the optical detection under different cases.

1. INTRODUCTION

Metamaterials, as a new artificial material, due to their special optical properties like negative refraction [1–4], anisotropic material properties [5, 6] and strong light-matter interaction [7–12], have drawn more and more attention in electromagnetic fields. Using metamaterials and metasurfaces to control and manipulate electromagnetic waves would result in a large number of applications, such as optical imaging [13–17], cloaking [18–20], optical interconnect [21, 22], and computing [23–25]. Conventional optical information processing systems are usually bulky and complicated, so new compact and efficient designs are always in search. Researches about using optical metamaterials to achieve mathematical operations have been done widely [23, 26–30]. For example, optical differentiation, including the first and second differential, has been realized either using Fourier optical system or Green-function films, which could be applied to optical edge-detection.

Current researches on edge detection using optical differentiation are usually based on two basic configurations: Fourier-plane based phase modulation and Green-function approach based multi-layers [23]. However, both of them have the limitations on the theoretical design and practical applications. First, the Fourier-plane approach is always bulky and complicated, since it needs to build an optical system, including lens, to realize the optical edge detection. However, the idea of integration is deeply rooted in the scientific community and industry, where thinner and lighter systems are highly desired instead of bulky ones. Second, recent Green-function approach based optical edge

Received 14 June 2022, Accepted 17 August 2022, Scheduled 22 August 2022

* Corresponding author: Hongsheng Chen (hansomchen@zju.edu.cn), Haoliang Qian (haoliangqian@zju.edu.cn).

[1] Interdisciplinary Center for Quantum Information, State Key Laboratory of Modern Optical Instrumentation, ZJU-Hangzhou Global Scientific and Technological Innovation Center, Zhejiang University, Hangzhou 310027, China. [2] International Joint Innovation Center, Key Lab. of Advanced Micro/Nano Electronic Devices & Smart Systems of Zhejiang, The Electromagnetics Academy at Zhejiang University, Zhejiang University, Haining 314400, China. [3] Jinhua Institute of Zhejiang University, Zhejiang University, Jinhua 321099, China.

detection requires multiple designated layers. Since it is too difficult to do the inverse design of the metamaterials to behave certain functions, the increasing of the degree of freedom leads to rather great difficulties on design. In recent years, with the continuous development of artificial intelligence, it has been verified that deep learning is a helpful and effective method to solve and optimize various complex and difficult problems. Previous research has proved that deep learning, as a rapid and efficient method, could dramatically increase the design speed of metasurface [31–35]. Thus, considering the complexity of Green-function film design, it could be an effective means to use deep learning to design films that display optical differentiation, which will simplify the design process and lower the requirements for designers.

It has been known that if one would like to realize the optical differentiation, it is vital to make the reflectivity or transmittivity of the films follow certain regular rules, that is, the larger the incident angle is, the higher reflectivity or transmittivity the films have. However, it could be a challenge for classical materials to behave like that unless multiple layers with designed material properties are fabricated. To cross this dilemma, epsilon-near-zero (ENZ) material [36, 37] is proposed here to realize such optical differentiation with much simpler configuration. The epsilon of such material is close to zero, which could generate the desired angle-dependent reflectivity as required by the optical edge detection. Therefore, it is suggested that even only one layer of ENZ material could possibly perform the optical differentiation.

Thus, with the help of deep learning, we use the ENZ material to design the Green-function approach based optical films, which could realize both the 1^{st}, 1.5^{th}, 2^{nd} optical differentiation under coherent incident light with p-polarization and the optical edge-detection under both coherent light with random polarization, where we use half p- and half s-polarization as one representative, and incoherent incident light cases. In this article, we will first introduce the ENZ material and then explain why it is our choice. After that, deep learning design algorithm and process will be presented, together with the predictive parameters of the ENZ films, including the thickness and the optical refractive index. Finally, different orders of differentiation under coherent incident light with p-polarized conditions is investigated in details, as well as the optical edge-detection on both coherent incident light with half p- and half s-polarized conditions and incoherent incident light cases.

2. BASIC DESIGN AND THEORETICAL MODELING

In order to achieve the function of optical differentiation, we choose the ENZ materials whose permittivity is close to zero, and we will explain it in the followings. According to the boundary condition for the electromagnetic field, when the epsilon of the material is small, its corresponding magnitude of the perpendicular component of the electric-field would be large. It means that only when the incident angle is small, impendence-mismatch would be less because there is less perpendicular component of the electric field than the parallel component. Thus, we make a conclusion that, for ENZ

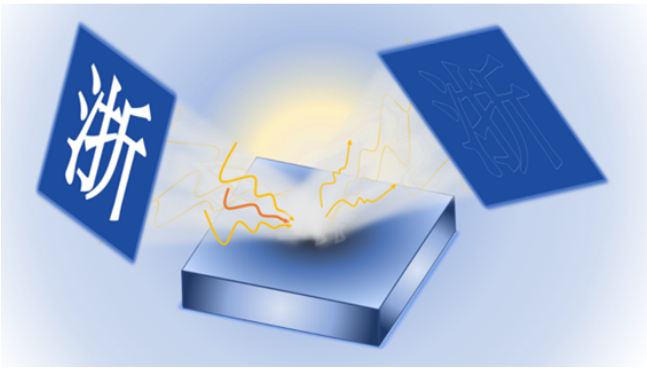

Figure 1. The film to realize optical edge-detection. The ENZ layer is used as the film to realize the optical edge detection. With the unique optical properties of ENZ, if the angle of incident light is larger, the corresponding reflection coefficient would be higher, which is associated with the high momentum signal in the angular spectrum representation.

material, the smaller the incident angle is, the less light would be reflected, which nicely meets our requirement of optical differentiation — smaller angle, smaller reflectance.

Here, we use these ENZ materials to design our film structure. When light enters from one side of the film, due to the ENZ property, the light with large incident angle would be reflected with higher coefficient. Since the edge of the picture belongs to the high momentum signal, according to the angular spectrum representation, it is related to the parts with larger angles in the angular spectrum. On the basis of the analysis before, we would have the edge of the image dominating the reflection as shown in Fig. 1, which realize the optical edge-detection. And in this work, by using ENZ materials with different permittivities, we could achieve different differential behaviors.

3. RESULTS

As we have described before, it is difficult to do the inverse design for the Green-function based film structure directly. Thus, deep learning is utilized to help the design and optimize the structure. We first consider the 1^{st}, 2^{nd}, and 1.5^{th} order of differential using one-layer film under coherent light incidence with p-polarized conditions. We build a net that has 10 input neurons and 3 output neurons, standing for the reflectance under different incident angles (the reflectivity is taken every 9 degrees from 0 degree to 81 degree) and the parameters (thickness, n and k) of the film respectively. The net structure is shown in Fig. 2(a) in details. Here, we ignore the incident angle that is larger than 81 degrees because of the limitation of the visual field of the human eye. We train the net until the loss is close to 0.01. Since the picture could be mapped to the angular spectrum using the Fourier transform, the objective functions of different orders of the differentiation, which is similar to different orders of the delta function, could be expressed by the n-th power of trigonometric functions in angular spectrum [38], where n represents the differentiation's order. Thus, we generate the data of the 1^{st} and 2^{nd} order of differentiation from two functions, $y = \sin(x)$ and $y = \sin^2(x)$, and consider it as the standard differential data of the net's output. Then we input the differentiation data into the trained net to predict the film structure. The parameters of the film under different orders of the differentiation are shown in Table 1, and the corresponding reflectances for the 1^{st} and 2^{nd} differential are shown in Figs. 2(b)–(c). It is found that, within the limits of error, both predicted reflectances are close to the standard differentiation curve and considered capable of 1^{st} and 2^{nd} differential. Also, note that the higher the order of the differentiation is, the steeper the incident angle-reflectance curve is. Therefore, by adjusting the parameters of the ENZ material, we could get the corresponding curve as different orders of the differentiation.

Table 1. The prediction of our net for the parameters of the ENZ material.

	h (nm)	n	k
1 order	25.3665	0.0584	0.1218
1.5 order	24.1672	0.0774	0.1388
2 order	22.7166	0.1003	0.1593

Then we use this predicted film to simulate the reflected image under coherent Gaussian light incidence with p-polarized conditions. The results are shown in Fig. 3. The difference between the 1^{st} and 2^{nd} differentiation for an image is mainly embodied in the following aspects. First, though both the 1^{st} and 2^{nd} differentials could realize optical edge detection, the edge for the 2^{nd} differential could be thinner than that for the 1^{st} differential. Second, the 1^{st} differential is more sensitive to the stair image, while the 2^{nd} differential is more sensitive to the details of the image. Therefore, we can see that in our results, the edge in Fig. 3(c) would be thinner than that in Fig. 3(b), and the details in Fig. 3(f) would be much clearer than those in Fig. 3(e). Thus, we conclude that our simulation results are exactly the results of the 1^{st} and 2^{nd} order differentials, which means that our film structure could realize the 1^{st} and 2^{nd} differentiation of the optical image under p-polarized incident light.

Furthermore, in order to achieve optical differentiation under both coherence incident light with half p- and half s-polarization and incoherence incident light, where both half p- and half s-polarized

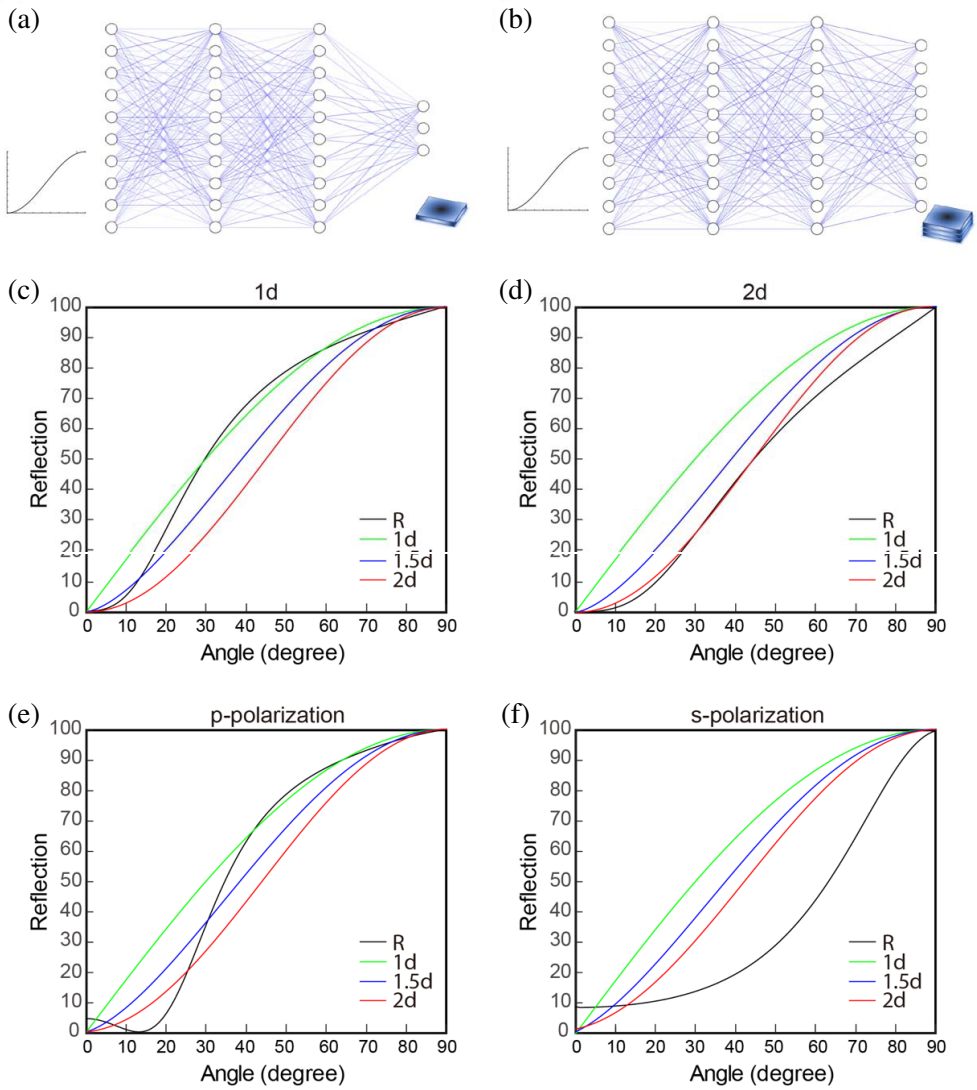

Figure 2. Net structures and corresponding predictions. (a), (b) The net structures are trained under two cases: one is coherent light incident with p-polarized conditions, and the other is coherent light incident with half p- and half s-polarization and incoherent incident light. For these two net structures, the number of input neurons is the same while the number of output neurons is different, since the number of reflection angles are taken the same while the parameters for the two film structures are different. (c), (d) The predicted reflectance of 1^{st}- and 2^{nd}-differential under coherent light incident with p-polarized conditions. (e), (f) The predicted reflectance under coherent incident light with half p- and half s-polarization and incoherent incident light. The black line is the predicted reflectance, and the green, blue, red line is the reflectance with standard reflectance with 1^{st}, 1.5^{th}, 2^{nd} differentiation, respectively.

components of the incident light are required to have the similar differentiation behavior we mentioned before. We train a new net whose detailed structure is shown in Fig. 2(d), which has 10 input neurons standing for the reflectance and 8 output neurons standing for the parameters of three-layers ENZ films. Here, we assume that the k (extinction coefficient of the refractive index) of the first layer is zero, thus it is not set in the net. We also train the net and get the final loss close to 0.01. The corresponding standard differential reflectance, which is generated as what we showed before, is inputted to the trained net. The predicted parameters of three-layer structure are shown in Table 2, and the corresponding reflectances are shown in Figs. 2(e)–(f). For p-polarized light, the predicted reflectance is in the area

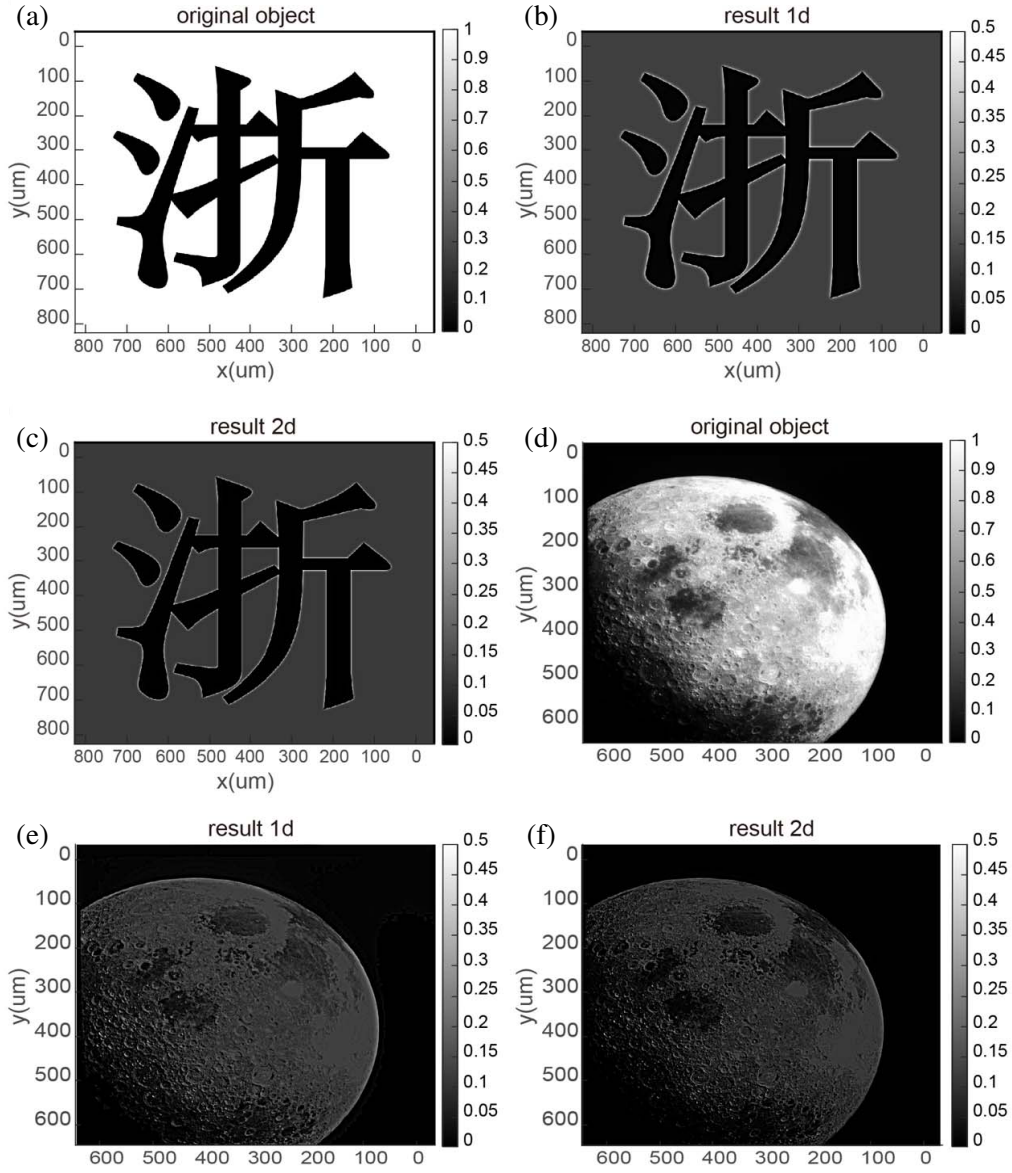

Figure 3. The simulation results, which are done under coherent cases with p-polarized incident light whose wavelength is 600 nm, of 1st- and 2nd-differential respectively. (a), (d) The original pictures. (b), (e) The corresponding results under 1st-differential. (c), (f) The corresponding results under 2nd-differential.

between 1st and 2nd differential curves. It means that the film could realize optical differentiation whose order is between 1st and 2nd, which could be regarded as successful optical differentiation to realize optical edge detection. Also, for s-polarized incident light, the predicted reflectance is close to the zone bounded with the standard 1st and 2nd order of differentiation. Since the differentiation curve in Fig. 2(f) would be closer to the x-axis if the order of differentiation is higher, the predicted reflectance (black curve in Fig. 2(f)) still represents optical differentiation but of a higher order, so the error between our reflectance and the bounded zone is thought acceptable for our edge detection system.

Then we use the predicted film structure to do the simulation under both the coherent incident Gaussian light with half p- and half s-polarized conditions and incoherent incident Gaussian light. According to differentiation curve under the half p- and half s-polarized lights, we first calculate these two components of the incident light respectively and then get the reflected results of the coherent and

Table 2. The prediction of our net for the parameters of the material on different layers.

	T (nm)	n	k
1	12.094	2.8861	0
2	58.894	0.019955	0.41657
3	29.237	2.3934	0.013536

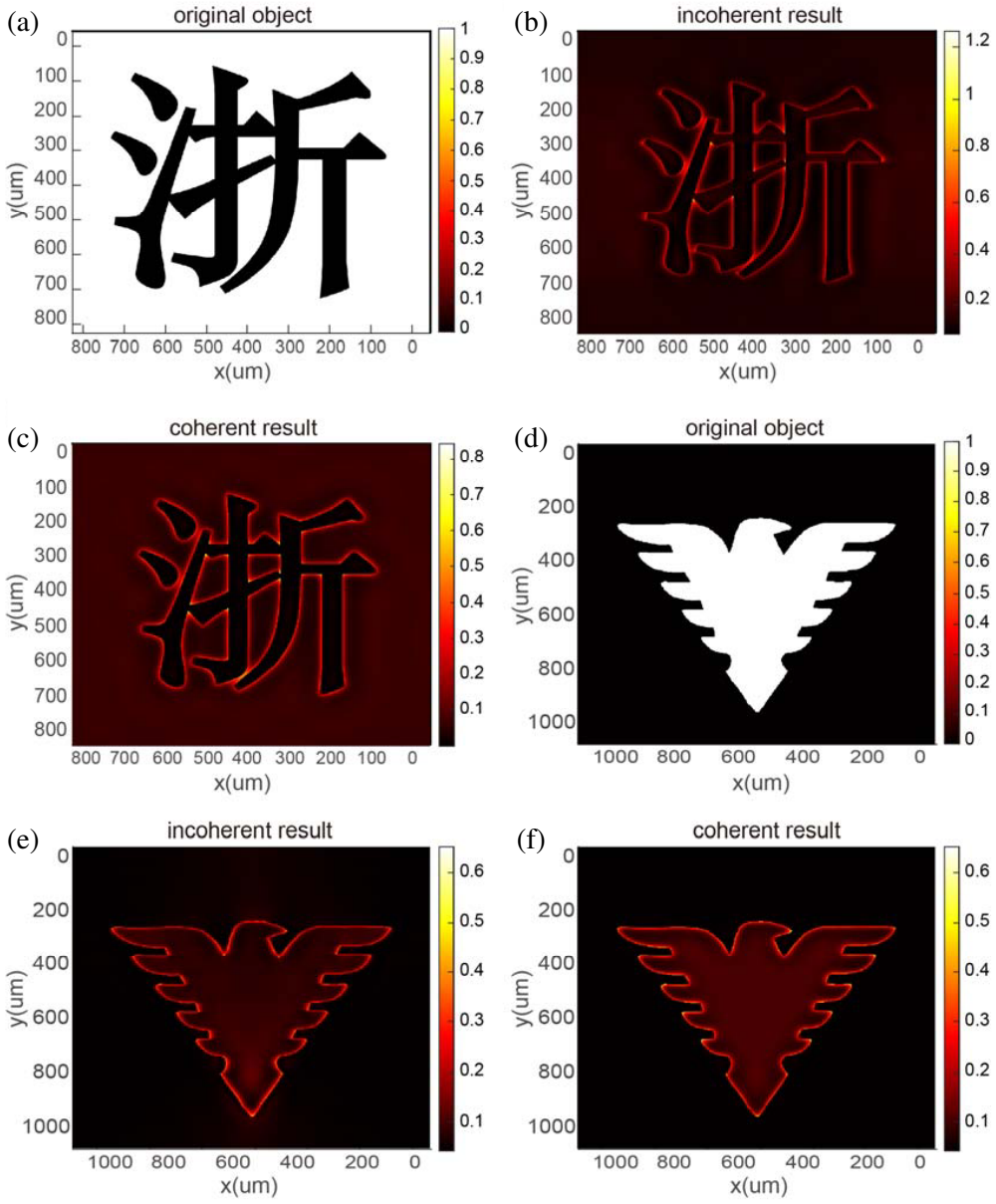

Figure 4. The simulation results, which are done under coherent light with half p- and half s-polarization and incoherent light whose wavelength is 600 nm respectively. (a), (d) The original pictures. (b), (e) The corresponding results under coherence light. (c), (f) The corresponding results under incoherence light.

incoherent incident light. The corresponding reflected images are shown in Fig. 4. For coherent light, when calculating its angular spectrum, we assume that the amplitudes of the half p- and half s-polarized components are the same, while for incoherent light, the amplitudes of the half p- and half s-polarized components are calculated according to the position on the receiving plane. The results show that, using our film structure, both the coherent and incoherent incident lights could achieve the edge detection.

4. DISCUSSION AND CONCLUSION

In our work, we have considered two different aspects of optical differentiation. First, we focused on the performance of a specific order of differentiation, such as the 1^{st} and 2^{nd} order. And second, we focused on the differential performance on both the half p- and half s-polarized lights. Furthermore, it could be a solution to increase the number of film layers, enabling much more complicated refractive index distribution for the desired performance. Besides, the structure we mentioned in this paper could be fabricated by film deposition. The different refractive indices could be achieved by different doping levels of transparent conductive oxide [39].

In this paper, we propose a new material-ENZ material, to design the Green-function based film structures to realize the optical differentiation and moreover, achieve the optical edge detection. To overcome the film-design problem, we use the deep learning method to greatly reduce the difficulty of design. Two net structures are built in our work for two different film structures and are trained until the satisfactory loss appears. Then we get the predicted film parameters and the corresponding reflectance under two different differential situations — the different orders, the 1^{st} and 2^{nd}, of differentiation, and the optical differentiation under both half p- and half s-polarized lights — and compare them with the standard reflectance we want. When ignoring the acceptable error, our prediction meets the need of optical differentiation. Furthermore, we use the predicted parameters of the film structures to do the simulation under coherent incident light with p-polarized conditions, coherent light cases incident with half p- and half s-polarized conditions and incoherent light cases. The results confirm that both of our films generated from two different net structures could realize optical edge detection. The film we design here is deep subwavelength and thus overcomes the problem of Fourier-plane based phase modulation, whose system is always bulky and complex. Our research shows an easy approach to design the Green-function film for optical differentiation, and suggests that the ENZ material could do optical edge detection easily.

ACKNOWLEDGMENT

The work at Zhejiang University was sponsored by the National Key Research and Development Program of China under Grant 2021YFB2801801, and the National Natural Science Foundation of China (NNSFC) under Grants No. 62005237, Grants No. 62175217.

Author Contributions

H.Q. conceived the idea. Y.S. conducted the numerical modeling and simulations. Y.S., Y.F., and H.Q. contributed extensively to the writing of the manuscript. Y.S., Y.F., Y.Z., H.C., and H.Q. analyzed data and interpreted the details of the results. H.C. and H.Q. supervised the research.

Declaration of Competing Interest

The authors declare no competing interests.

Data Availability Statement

The data that supports the plots within this letter and other findings of this study are available from the corresponding author upon reasonable request.

REFERENCES

1. Smith, D. R., J. B. Pendry, and M. C. K. Wiltshire, "Metamaterials and negative refractive index," *Science*, Vol. 305, 788–792, 2004.
2. Pendry, J. B., "Negative refraction makes a perfect lens," *Phys. Rev. Lett.*, Vol. 85, 3966, 2000.
3. Tsakmakidis, K. L., A. D. Boardman, and O. Hess, "Trapped rainbow storage of light in metamaterials," *Nat.*, Vol. 450, 397–401, 2007.
4. Hoffman, A. J., L. Alekseyev, S. S. Howard, K. J. Franz, D. Wasserman, V. A. Podolskiy, E. E. Narimanov, D. L. Sivco, and C. Gmachl, "Negative refraction in semiconductor metamaterials," *Nat. Mater.*, Vol. 6, 946–950, 2007.
5. Jiang, W. X., J. Y. Chin, and T. J. Cui, "Anisotropic metamaterial devices," *Mater. Today*, Vol. 12, 26–33, 2009.
6. Iyer, A. K., D. Pratap, J. G. Pollock, and S. A. Ramakrishna, "Anisotropic metamaterial optical fibers," *Opt. Express*, Vol. 23, 9074–9085, 2015.
7. Zeng, Y., H. Qian, M. J. Rozin, Z. Liu, and A. R. Tao, "Enhanced second harmonic generation in double-resonance colloidal metasurfaces," *Adv. Funct. Mater.*, Vol. 28, 1803019, 2018.
8. Qian, H., "Efficient light generation from enhanced inelastic electron tunnelling," *Nat. Photonics*, Vol. 12, 485–488, 2018.
9. Lu, D., H. Qian, K. Wang, H. Shen, F. Wei, Y. Jiang, E. E. Fullerton, P. K. L. Yu, and Z. Liu, "Nanostructuring multilayer hyperbolic metamaterials for ultrafast and bright Green InGaN quantum wells," *Adv. Mater.*, Vol. 30, 1706411, 2018.
10. Ghobadi, A., H. Hajian, B. Butun, and E. Ozbay, "Strong light-matter interaction in lithography-free planar metamaterial perfect absorbers," *ACS Photonics*, Vol. 5, 4203–4221, 2018.
11. Galfsky, T., J. Gu, E. E. Narimanov, and V. M. Menon, "Photonic hypercrystals for control of light-matter interactions," *Proc. Natl. Acad. Sci. U.S.A.*, Vol. 114, 5125–5139, 2017.
12. Krishnamoorthy, H. N. S., Z. Jacob, E. Narimanov, I. Kretzschmar, and V. M. Menon, "Topological transitions in metamaterials," *Science*, Vol. 336, 205–209, 2012.
13. Banerji, S., M. Meem, A. Majumder, F. G. Vasquez, B. Sensale-Rodriguez, and R. Menon, "Imaging with flat optics: Metalenses or diffractive lenses?" *Opt.*, Vol. 6, No. 6, 805–810, 2019.
14. Lu, D. and Z. Liu, "Hyperlenses and metalenses for far-field super-resolution imaging," *Nat. Commun.*, Vol. 3, 1–9, 2012.
15. Liu, Z., H. Lee, Y. Xiong, C. Sun, and X. Zhang, "Far-field optical hyperlens magnifying sub-diffraction-limited objects," *Science*, Vol. 315, 1686, 2007.
16. Ma, Q., H. Qian, S. Montoya, et al., "Experimental demonstration of hyperbolic metamaterial assisted illumination nanoscopy," *ACS Nano*, Vol. 12, 11316–11322, 2018.
17. Smolyaninov, I. I., Y. J. Hung, and C. C. Davis, "Imaging and focusing properties of plasmonic metamaterial devices," *Phys. Rev. B*, Vol. 76, 205424, 2007.
18. Pendry, J. B., D. Schurig, and D. R. Smith, "Controlling electromagnetic fields," *Science*, Vol. 312, 1780–1782, 2006.
19. Cai, W., U. K. Chettiar, A. V. Kildishev, and V. M. Shalaev, "Optical cloaking with metamaterials," *Nat. Photonics*, Vol. 1, 224–227, 2007.
20. Schurig, D., J. J. Mock, B. J. Justice, S. A. Cummer, J. B. Pendry, A. F. Starr, and D. R. Smith, "Metamaterial electromagnetic cloak at microwave frequencies," *Science*, Vol. 314, 977–980, 2006.
21. Fang, Y. and M. Sun, "Nanoplasmonic waveguides: Towards applications in integrated nanophotonic circuits," *Light Sci. Appl.*, Vol. 4, e294–e294, 2015.
22. Liu, Y., J. Zhang, H. Liu, S. Wang, and L. M. Peng, "Electrically driven monolithic subwavelength plasmonic interconnect circuits," *Sci. Adv.*, Vol. 3, e1701456, 2017.
23. Navon, N., S. Nascimbène, F. Chevy, and C. Salomon, "Performing mathematical operations with metamaterials," *Science*, Vol. 343, 729–732, 2014.
24. Zangeneh-Nejad, F., D. L. Sounas, A. Alù, and R. Fleury, "Analogue computing with metamaterials," *Nat. Rev. Mater.*, Vol. 6, 207–225, 2020.

25. Cheng, K., Y. Fan, W. Zhang, Y. Gong, S. Fei, and H. Li, "Optical realization of wave-based analog computing with metamaterials," *Appl. Sci.*, Vol. 11, 141, 2020.
26. Zhou, J., S. Liu, H. Qian, et al., "Metasurface enabled quantum edge detection," *Sci. Adv.*, Vol. 6, 4385–4401, 2020.
27. Zhou, J., H. Qian, J. Zhao, M. Tang, Q. Wu, M. Lei, H. Luo, S. Wen, S. Chen, and Z. Liu, "Two-dimensional optical spatial differentiation and high-contrast imaging," *Natl. Sci. Rev.*, Vol. 8, No. 6, nwaa176, 2021.
28. Zhou, J., H. Qian, C.-F. Chen, and Z. Liu, "Optical edge detection based on high-efficiency dielectric metasurface," *Proc. Natl. Acad. Sci.*, Vol. 166, 11137–11140, 2019.
29. Zhou, J., H. Qian, H. Luo, S. Wen, and Z. Liu, "A spin controlled wavefront shaping metasurface with low dispersion in visible frequencies," *Nanoscale*, Vol. 11, 17111–17119, 2019.
30. Zhou, J., H. Qian, G. Hu, H. Luo, S. Wen, and Z. Liu, "Broadband photonic spin hall meta-lens," *ACS Nano*, Vol. 12, 82–88, 2018.
31. Kiarashinejad, Y., S. Abdollahramezani, M. Zandehshahvar, O. Hemmatyar, and A. Adibi, "Deep learning reveals underlying physics of light-matter interactions in nanophotonic devices," *Adv. Theory Simulations*, Vol. 2, 1900088, 2019.
32. Malkiel, I., M. Mrejen, A. Nagler, U. Arieli, L. Wolf, and H. Suchowski, "Plasmonic nanostructure design and characterization via deep learning," *Light Sci. Appl.*, Vol. 7, 1–8, 2018.
33. An, S., C. Fowler, B. Zheng, M. Y. Shalaginov, et al., "A deep learning approach for objective-driven all-dielectric metasurface design," *ACS Photonics*, Vol. 6, 3196–3207, 2019.
34. Qiu, T., X. Shi, J. Wang, Y. Li, S. Qu, Q. Cheng, T. Cui, and S. Sui, "Deep learning: A rapid and efficient route to automatic metasurface design," *Adv. Sci.*, Vol. 6, 1900128, 2019.
35. Kiarashinejad, Y., M. Zandehshahvar, S. Abdollahramezani, O. Hemmatyar, R. Pourabolghasem, and A. Adibi, "Knowledge discovery in nanophotonics using geometric deep learning," *Adv. Intell. Syst.*, Vol. 2, 1900132, 2020.
36. Campione, S., S. Liu, A. Benz, J. F. Klem, M. B. Sinclair, and I. Brener, "Epsilon-near-zero modes for tailored light-matter interaction," *Phys. Rev. Appl.*, Vol. 4, 044011, 2015.
37. Niu, X., X. Hu, S. Chu, and Q. Gong, "Epsilon-near-zero photonics: A new platform for integrated devices," *Adv. Opt. Mater.*, Vol. 6, 1701292, 2018.
38. Son, H. and K. Oh, "Light propagation analysis using a translated plane angular spectrum method with the oblique plane wave incidence," *J. Opt. Soc. Am. A*, Vol. 32, 949, 2015.
39. Wang, Z., C. Chen, K. Wu, H. Chong, and H. Ye, "Transparent conductive oxides and their applications in near infrared plasmonics," *Phys. Status Solidi*, Vol. 216, 1700794, 2019.